Circulation

ORIGINAL RESEARCH ARTICLE

Myocardial Gene Expression Signatures in Human Heart Failure With Preserved Ejection Fraction

BACKGROUND: Heart failure (HF) with preserved ejection fraction (HFpEF) constitutes half of all HF but lacks effective therapy. Understanding of its myocardial biology remains limited because of a paucity of heart tissue molecular analysis.

METHODS: We performed RNA sequencing on right ventricular septal endomyocardial biopsies prospectively obtained from patients meeting consensus criteria for HFpEF (n=41) contrasted with right ventricular septal tissue from patients with HF with reduced ejection fraction (HFrEF, n=30) and donor controls (n=24). Principal component analysis and hierarchical clustering tested for transcriptomic distinctiveness between groups, effect of comorbidities, and differential gene expression with pathway enrichment contrasted HF groups and donor controls. Within HFpEF, non–negative matrix factorization and weighted gene coexpression analysis identified molecular subgroups, and the resulting clusters were correlated with hemodynamic and clinical data.

RESULTS: Patients with HFpEF were more often women (59%), African American (68%), obese (median body mass index 41), and hypertensive (98%), with clinical HF characterized by 65% New York Heart Association Class III or IV, nearly all on a loop diuretic, and 70% with a HF hospitalization in the previous year. Principal component analysis separated HFpEF from HFrEF and donor controls with minimal overlap, and this persisted after adjusting for primary comorbidities: body mass index, sex, age, diabetes, and renal function. Hierarchical clustering confirmed group separation. Nearly half the significantly altered genes in HFpEF versus donor controls (1882 up, 2593 down) changed in the same direction in HFrEF; however, 5745 genes were uniquely altered between HF groups. Compared with controls, uniquely upregulated genes in HFpEF were enriched in mitochondrial adenosine triphosphate synthesis/electron transport, pathways downregulated in HFrEF. HFpEF-specific downregulated genes engaged endoplasmic reticulum stress, autophagy, and angiogenesis. Body mass index differences largely accounted for HFpEF upregulated genes, whereas neither this nor broader comorbidity adjustment altered pathways enriched in downregulated genes. Non–negative matrix factorization identified 3 HFpEF transcriptomic subgroups with distinctive pathways and clinical correlates, including a group closest to HFrEF with higher mortality, and a mostly female group with smaller hearts and proinflammatory signaling. These groupings remained after sex adjustment. Weighted gene coexpression analysis yielded analogous gene clusters and clinical groupings.

CONCLUSIONS: HFpEF exhibits distinctive broad transcriptomic signatures and molecular subgroupings with particular clinical features and outcomes. The data reveal new signaling targets to consider for precision therapeutics.

Virginia S. Hahn, MD*
Hildur Knutsdottir, PhD*
Xin Luo, PhD
Kenneth Bedi, BS
Kenneth B. Margulies, MD
Saptarsi M. Haldar, MD
Marina Stolina, PhD
Jun Yin, PhD
Aarif Y. Khakoo, MD
Joban Vaishnav, MD
Joel S. Bader, PhD
David A. Kass, MD
Kavita Sharma, MD

*Drs Hahn and Knutsdottir contributed equally.

Key Words: computational biology ■ heart failure ■ humans ■ sequence analysis, RNA

Sources of Funding, see page 133

https://www.ahajournals.org/journal/circ

Clinical Perspective

What Is New?

- We performed myocardial transcriptomic analysis in heart failure with preserved ejection fraction (HFpEF), heart failure with reduced ejection fraction (HFrEF), and controls.
- Upregulated genes in oxidative phosphorylation pathways in HFpEF were associated with obesity, whereas downregulated genes in endoplasmic reticulum stress, autophagy, and angiogenesis were independent of comorbidities.
- We identified a HFpEF subgroup with a transcriptomic signature more similar to HFrEF. This group had larger hearts, worse pulmonary hypertension, higher NT-proBNP (N-terminal pro–B-type natriuretic peptide), and worse clinical outcomes.

What Are the Clinical Implications?

- Transcriptome-derived HFpEF subgroups include one more similar to HFrEF that may benefit from proven HFrEF therapies and others that may benefit from targeted therapies addressing inflammation, proteostasis, and angiogenesis.

Heart failure (HF) with preserved ejection fraction (HFpEF) affects about half of all patients with HF, affecting >13 million adults worldwide.[1] Patients develop symptoms similar to those of HF with reduced ejection fraction (HFrEF), having high hospitalization rates, morbidity, and mortality.[2,3] Unlike HFrEF, effective therapies for HFpEF are lacking. The past 2 decades have witnessed a transformation of HFpEF phenotypes from mostly hypertensive cardiac hypertrophy with diastolic dysfunction[4,5] to a syndrome marked by severe obesity and associated comorbidities.[6–8] The heterogeneity of HFpEF—from its clinical presentation to comorbidities—is inculpated in the disappointing efforts to uncover successful treatment.[9] Little remains understood about the underlying biology of HFpEF, and although animal models can be helpful, they struggle to capture the multidimensionality of this syndrome.

One likely reason human HFpEF remains a clinical and therapeutic conundrum is that so little is known about its underlying molecular biology given the paucity of tissue harvesting. Existing heart data stem from small cohorts of mostly hypertensive patients with left ventricular (LV) hypertrophy, some with diffuse coronary disease, but with minimal obesity.[10–13] Tissue biopsies revealed a stiff myocardium from fibrosis and titin modifications,[5,10] increased inflammatory markers,[11] and reduced protein kinase G activity.[12] Gene expression profiling has not been reported to date in a prospectively defined HFpEF cohort; thus, whether there is a distinctive HFpEF signature despite clinical heterogeneity, whether and how it is altered by obesity and other comorbidities, and whether a molecular phenotype can identify clinical HFpEF subgroups are unknown.

We assessed gene expression profiles in patients with HFpEF in comparison with patients with HFrEF and donor controls to test the hypotheses that (1) despite clinical heterogeneity, patients with HFpEF exhibit a distinctive gene transcriptome that contrasts with that of patients with HFrEF and controls; (2) these differences involve enriched pathways with strong association as well as independence from major comorbidities such as obesity; and (3) molecular phenotyping can identify HFpEF subgroups that exhibit distinct clinical features and prognosis. Our ultimate goal was to identify a transcriptomic signature of subsets of patients with HFpEF that may ultimately lead to improved personalized therapeutics.

METHODS

Data Sources

The following items are posted in an online data repository[14]: raw mapped reads for all identified genes for each patient; normalized read counts for these genes based on DESeq analysis; the primary data set we used in our analysis that has median reads and between-group statistical analysis for genes that pass our noise-level filter (see following) for each patient group; data in a similar format but pertaining to HFpEF subgroups; and metadata with patient identification number to reference with the gene databases, tissue source (eg, right versus left heart, site), and disease group.

HFpEF Study Population

The HFpEF patient group consisted of those referred to the Johns Hopkins University HFpEF clinic from January 2016 through April 2018 who provided informed consent for an endomyocardial biopsy research protocol as approved by the Johns Hopkins institutional review board. All patients underwent clinical assessment, echocardiography, and invasive hemodynamic testing. HFpEF diagnostic criteria were based on current guideline definitions of HFpEF[15–17] to include the following: signs and symptoms of clinical HF using Framingham criteria for HF,[18] LV ejection fraction ≥50% by echocardiography within the previous 12 months, and at least 2 of the following: (1) structural heart disease (increased LV wall thickness or left atrial diameter) or diastolic dysfunction on echocardiography[19]; (2) NT-proBNP (N-terminal pro–B-type natriuretic peptide) ≥125 pg/mL; or (3) hemodynamic evidence of elevated left-sided filling pressures (pulmonary artery wedge pressure ≥15 mm Hg at baseline or ≥25 mm Hg with exercise). Exclusion criteria included history of LV ejection fraction <40%, HF with midrange ejection fraction (40% to 50%), greater than moderate valvular disease, infiltrative cardiomyopathy (including cardiac amyloidosis), restrictive cardiomyopathy, congenital heart disease, constrictive pericarditis, isolated pulmonary arterial hypertension, hypertrophic cardiomyopathy (known genetic variant, severe unexplained LV hypertrophy, or presence of myocyte disarray

on histology), or heart transplantation. Data are generally reported as median (25th, 75th percentiles).

Myocardial Tissue Procurement and Processing

Patients with HFpEF (n=63) underwent right heart catheterization with endomyocardial biopsy (Jawz Bioptome, Argon Medical, Frisco, TX) in the supine position through internal jugular venous access and echocardiographic guidance, which we have described previously. A total of 7 to 9 right ventricular (RV) septal biopsies were obtained: 3 or 4 for clinical histology and the remainder rapidly frozen in liquid nitrogen for analysis. Clinical histology for myocyte hypertrophy and fibrosis was assessed by a cardiovascular pathologist. Quantitative analysis of myocardial fibrosis and CD68+ cell count was performed as previously described.[20] Briefly, fibrosis (Masson trichrome) and myocyte hypertrophy (hematoxylin and eosin) were qualitatively graded by a cardiovascular pathologist and provided in the clinical report. Quantitative analysis of fibrosis (Masson trichrome) and CD68+ cell number (immunohistochemistry) was performed using HALO (Area Quantification FL Algorithm, Indica Laboratory, Albuquerque, NM). Biopsies positive for cardiac amyloidosis based on Congo red staining (n=7) were excluded. RNA was isolated from 48 of the remaining samples with sufficient tissue, with RNA suitable for sequencing obtained in 41.

HFpEF biopsies were compared with RV midseptal myocardium obtained from brain-dead organ donors (controls, n=24) and from HFrEF explanted hearts (n=30) in patients undergoing transplantation. HFrEF and control tissues were provided from the University of Pennsylvania under an institutional review board–approved protocol. LV septal tissue from the same hearts was also obtained. The deidentified clinical/demographic data from these participants were determined close to time of death (controls) or cardiac transplantation.

RNA Isolation and Preparation

Samples were crushed using a disposable pellet pestle (Kimble Chase, Vineland, NJ) in 150 µL of Buffer RLT with 1% BME (Qiagen, Germantown, MD) then homogenized in a Magna Lyser (Roche Diagnostics, Indianapolis, IN) for 30 seconds at 6500 rpm. After homogenization, 298 µL of RNAase-free water and 2 µL of a 50 mg/mL proteinase K solution were added to each tube and mixed well. Samples were incubated at 55°C for 10 minutes and centrifuged, and the supernatant was collected into a new 1.5 mL RNase-free microcentrifuge tube. RNA extraction was performed by using the RNeasy Micro Kit (Qiagen) with on-column DNase treatment (Qiagen) according to the manufacturer's instructions. RNA concentration and integrity were assessed using a nanoDrop 8000 (Thermo Fisher, Waltham, MA) and a Bioanalyzer (Agilent, Santa Clara, CA). Samples with ≥100 ng total RNA and RNA integrity numbers ≥7 were used for sequencing.

Analysis of Differential Gene Expression

The human genome was obtained in FASTA format (GRCh38) from Ensembl version 92 and gene set annotation in gtf format. The hisat2 indices were built from the genome index using hisat2-build[21] from Hisat2 version 2.1.0. Raw RNAseq paired-end reads were aligned to the genome using hisat2 (default flags). The total reads per sample ranged from 30 to 50 million and all sample alignment mapping rates were >97%. HTSeq was used to count reads mapping to individual genes by processing the sorted bam files with accepted read quality.[22]

DESeq2[23] was used to estimate differential gene expression among HFpEF, HFrEF, and control sample tissue starting with counts generated by HTSeq-count. Genes with a median read count <50 in each sample group or those with a high correlation (>0.5) to β-globin component of hemoglobin (from blood contamination in HFpEF biopsies) were excluded. Extreme expression outliers were detected and replaced based on the default Cook distance cutoff (99% quantile of the F[p,m–p] distribution, with *p* the number of parameters including the intercept and *m* number of samples). Gene expression was normalized using the DESeq2 median of ratios normalization. Differentially expressed genes were defined using the 5% false discovery rate (Benjamini-Hochberg method) threshold for significance. Adjustment for covariates was performed using generalized linear models within DESeq2. The full set of processed detected genes was first examined using principal component analysis (PCA) and unsupervised hierarchical cluster analysis. In clustering analysis, the variance stabilizing transform of the raw reads was used along with hierarchical clustering based on Pearson correlation. PCA was performed in R, using DEseq2 function plotPCA from the variance stabilizing transformation of the read counts. Gene pathway enrichment (Kyoto Encyclopedia of Genes and Genomes and gene ontology) was determined with clusterProfiler using R. Differential gene expression in specific pathways used Kyoto Encyclopedia of Genes and Genomes or BIO-RAD lists, calculating *Z* scores ([observed–mean]/SD) for each gene in the pathway comparing control with either HFpEF or HFrEF.

Weighted Correlation Network Analysis of HFpEF Samples

Weighted gene coexpression network analysis (WGCNA) was used to construct gene modules, based on correlation in expression levels in the HFpEF sample cohort.[24] The modules consist of functionally related genes and thus different modules tend to be involved in individual functions. Three patients (7709, 7715, and 7546) were excluded from this analysis based on low correlation with other HFpEF samples from sample–sample correlation analysis (Figure I in the Data Supplement). Using the HFpEF expression data (13 265 genes after the previously described low count and blood contamination filtering steps), a correlation matrix was created, which was transformed into a topologic overlap matrix using a signed network in the blockwiseModules function (using the following parameters: power 16 [selected from pickSoftThreshold cutoff of 0.95], minModuleSize 30, mergeCutHeight 0.25). Eight gene modules were identified, consisting of between 62 and 477 genes. Next, clinical traits were associated with each of the modules from their Pearson correlation with the module eigengenes (first principal component) calculated using the function moduleEigengenes. Lastly, a pathway analysis was conducted as described for each set of module genes.

Non–Negative Matrix Factorization to Identify Gene Expression–Based HFpEF Clusters

Non–negative matrix factorization (NMF) was used to determine whether there were transcriptional subgroups within the HFpEF patient samples.[25] NMF uses an iterative algorithm to detect a subset of features or genes to split the data into *k* groups. The same patient outliers from the WGCNA were excluded from this analysis (samples 7709, 7715, and 7546). Using the remaining 38 samples, the NMF Brunet algorithm detected 3 clusters (based on running NMF 40 times for each *k*=2,..,5, with a fixed initial seed and using cophenetic coefficient, a measure of robustness to select the optimum number of clusters).[26] The analysis was then repeated 250 times with *k*=3 with different initial conditions for model fitting. As per the NMF algorithm, metagenes for each of the 3 clusters were identified using consensus clustering. Differential gene expression was performed between controls and each HFpEF NMF subgroup individually. Clinical characteristics were compared among the 3 clusters of patients with HFpEF.

We performed Kaplan-Meier time-to-event analysis using both HF hospitalizations and deaths during 12 months of follow-up. We used a log-rank test to assess statistical significance among the curves of the 3 HFpEF groups (determined by NMF). Three patients were excluded because of very short follow-up (2 weeks to 2 months).

Statistical Analysis

Continuous data are generally reported as median (25th, 75th percentiles). Categorical data are generally reported as number (%). Significance threshold was determined by the 5% false discovery rate adjusted for multiple comparisons by the Benjamini-Hochberg method. Adjustment for covariates was performed using generalized linear models within DESeq2. Agnostic clustering was performed on variance stabilizing transform of the raw reads using PCA and unsupervised hierarchical clustering. Gene pathway enrichment was performed using a Fisher exact test of differentially expressed genes within the pathway of interest. Targeted pathway analysis compared *Z* scores for each gene in the pathway using Wilcoxon rank-sum test. WGCNA was performed excluding 3 outliers based on the sample–sample correlation analysis. Pearson correlation was used to determine clinical characteristics associated with each gene cluster. NMF was used to subgroup HFpEF. Kaplan-Meier time-to-event analysis with log-rank test was performed using the 3 transcriptomic subgroups determined by NMF. Events included HF hospitalizations and deaths. Kruskal-Wallis and Wilcoxon rank-sum tests were used for continuous variables and Fisher exact was used for categorical variables to compare clinical characteristics among groups.

RESULTS

Baseline Characteristics of Study Patients

Given the heterogeneity of patients with HFpEF, we provide a comprehensive characterization of clinical, echocardiographic, and invasive hemodynamic data of the study group (Table 1 and Table I in the Data Supplement). Their median age was 62 years, 59% were female, and 68% were Black, with a high burden of comorbidities, including hypertension (98%), diabetes (63%), and atrial fibrillation (24%). The median body mass index (BMI) was 40.8 kg/m^2 (range, 36 to 46). Clinical HF was evident with 70% having been hospitalized in the previous 1 year, 95% on loop diuretic therapy, and a median NT-proBNP of 169 pg/mL (range, 94 to 614) in this obese cohort. Echocardiography confirmed preserved ejection fraction, increased LV wall thickness, and diastolic dysfunction. Invasive hemodynamics revealed elevated right atrial and pulmonary artery pressures and a pulmonary artery wedge pressure median of 20 mm Hg (range, 15 to 24 mm Hg). Elevated pulmonary artery pressures were most often attributable to left-sided heart disease, with only 12% meeting criteria for precapillary pulmonary hypertension (pulmonary vascular resistance ≥3 Wood units). The group displayed substantial heterogeneity as seen in clinical practice with respect to systolic blood pressure, BMI, LV mass index, serum NT-proBNP, mean pulmonary artery pressure, and renal function (Figure II in the Data Supplement).

Table 1 provides additional data for control and HFrEF cohorts. These participants were younger, were more often White, less often had diabetes, had better renal function, and had a lower median BMI. Eighty percent of patients with HFrEF had nonischemic cardiomyopathy.

HFpEF, HFrEF, and Controls Have Distinct mRNA Expression Profiles

The filtered RNAseq read-set identified ≈13 000 genes. PCA using all RV septum expressed genes separated these into 3 distinct groups, with only a few overlapping patients in HFpEF and HFrEF (Figure 1A). PCA was also performed after first adjusting for sex only and sex plus the 4 other major covariates that differed between HFpEF and HFrEF: age, diabetes, BMI, and renal function (estimated glomerular filtration rate). The results show rotation of the vectors with a bit more overlap, but there is still clear separation of the groups (Figure 1B and Figure III in the Data Supplement). Unsupervised hierarchical cluster analysis (Figure 1C) also identified 3 distinct groupings, with 88% of HFpEF, 97% of HFrEF, and 100% of controls clustering within their category. Despite HFpEF clinical heterogeneity, the majority of genes exhibited a coefficient of variation among patients of <30% (23% [85% to 36%]), similar to HFrEF and controls (Figure IV in the Data Supplement). Because we had sampled the RV in all cases to match with HFpEF biopsy site, we also tested whether RV and LV septal transcripts correlate. This has been found in normal hearts[27]; here we examined

Table 1. Clinical Characteristics of HFpEF, HFrEF, and Donor Control Groups

Variable	Controls (n=24)	HFpEF (n=41)	HFrEF (n=30)	*P* value
Age, y	57 (52, 63)	62 (53, 69)†††	50 (45, 62)	0.003
Female	10 (42)	24 (59)	10 (33)	0.1
Race/ethnicity				<0.001
Black	1 (4)	28 (68)***, †††	8 (27)*	
White	22 (92)	11 (27)	21 (70)	
Hispanic	1 (4)	1 (2)	0 (0)	
Medications				
ACEi or ARB	6 (25)	26 (63)**	20 (67)**	0.003
β-Blocker	6 (25)	22 (54)*, †††	28 (93)***	<0.001
Loop diuretic	0 (0)	39 (95)***	30 (100)***	<0.001
Medical history				
Hypertension	11 (46)	40 (98)***	30 (100)***	<0.001
Diabetes	3 (12)	26 (63)***, †	9 (30)	<0.001
Coronary artery disease	1 (4)	4 (10)	5 (17)	0.36
Atrial fibrillation or flutter	3 (12)	10 (24)††	19 (63)***	<0.001
BMI, kg/m^2	27 (22, 31)	41 (36, 46)***, †††	26 (23, 29)	<0.001
eGFR, mL/min/1.73 m^2	83 (56, 104)	48 (33, 70)**, ††	70 (56, 82)	0.003
Cause of HFrEF				
Familial cardiomyopathy			6 (20)	
Ischemic heart disease			6 (20)	
Left ventricular noncompaction			2 (6.7)	
Non–ischemic dilated cardiomyopathy			15 (50)	
Sarcoidosis			1 (3.3)	
Echocardiography				
LVEF, %	61 (60, 65)	65 (60, 70)†††	18 (11, 20)***	<0.001
LVEDD, cm	4.0 (3.9, 4.5)	4.6 (4.0, 5.0)*, †††	6.8 (6.2, 7.3)***	<0.001
LV posterior wall, mm	9.5 (8.0, 11.0)	12.0 (9.7, 13.0)*, †††	8.55 (8.0, 10.0)	<0.001
Sex-adjusted LV mass/height$^{1.7}$, g/m$^{1.7}$	95 (86, 115)	107 (83, 131)†	121 (113, 150)**	0.004
LVMI, g/m^2	118 (97, 138)	95 (80, 119)**, †††	146 (131, 158)***	<0.001
Invasive hemodynamics				
RA, mm Hg	NA	12 (8, 15)††	7 (5, 11)	0.012
PASP, mm Hg	NA	45 (33, 54)	48 (40, 56)	0.68
PA mean, mm Hg	NA	29 (23, 35)	29 (23, 34)	0.55
PAWP, mm Hg	NA	20 (15, 24)	20 (16, 24)	0.94
Cardiac index, L/min/m^2	NA	2.52 (2.29, 3.09)†††	2.05 (1.80, 2.30)	<0.001
PVR ≥3 WU	NA	5 (12)	9 (30)	0.077
RA/PAWP ratio	NA	0.57 (0.50, 0.62)††	0.39 (0.27, 0.56)	0.002
PA pulsatility index	NA	2.0 (1.4, 2.7)†††	3.8 (2.8, 6.0)	<0.001

Data are n (%) or median (25th, 75th percentile). *P* value displayed for Fisher exact test was used for categorical variables, and Kruskal-Wallis test was used for continuous variables. Sex-adjusted left ventricular (LV) mass/height$^{1.7}$ was calculated by multiplying by a constant of 1.28 for women. Post hoc between-group comparison statistics (Wilcoxon) are as follows: *P<0.05 vs control, **P≤0.01 vs control, ***P≤0.001 vs control; †P<0.05 vs HFrEF, ††P≤0.01 vs HFrEF, †††P≤0.001 vs HFrEF. ACEi indicates angiotensin-converting enzyme inhibitor; ARB, angiotensin II receptor blocker; BMI, body mass index; eGFR, estimated glomerular filtration rate; HFpEF, heart failure with preserved ejection fraction; HFrEF, heart failure with reduced ejection fraction; LVEDD, left ventricular end-diastolic diameter; LVEF, left ventricular ejection fraction; LVMI, left ventricular mass index; NA, invasive hemodynamics not available for controls; PA, pulmonary artery; PASP, pulmonary artery systolic pressure; PAWP, pulmonary artery wedge pressure; PVR, pulmonary vascular resistance; and RA, right atrium.

HFrEF where tissue from both septal sides was obtained. We found an extremely high correlation of gene expression independent of presence or absence of pulmonary hypertension (Figure V in the Data Supplement). PCA and unsupervised hierarchical cluster analysis of RV and LV data from HFrEF and control

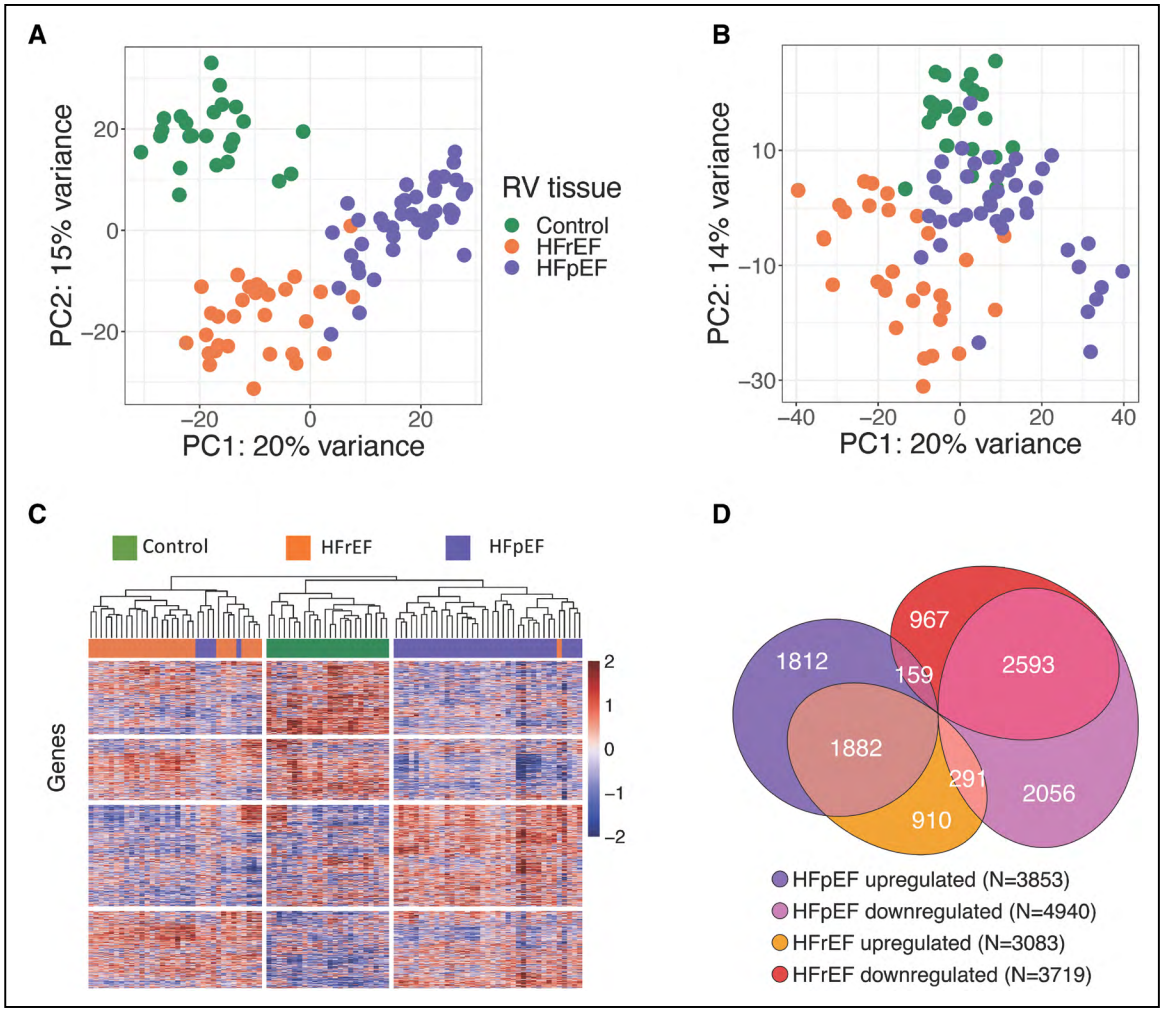

Figure 1. Transcriptomic differences between HFpEF and HFrEF.
RNAseq was performed on controls (n=24), HFrEF (n=30), and HFpEF (n=41). **A**, Principal component (PC) analysis using all identified genes for controls (green), HFrEF (orange), and HFpEF (purple) reveals within-group clusters with minimal overlap. **B**, PC analysis after adjustment for age, sex, diabetes, body mass index, and estimated glomerular filtration rate. **C**, Hierarchical clustering analysis using all identified genes, using Pearson correlation, shown as a heatmap of variance stabilizing transforms of the reads that also largely separates the groups. Only 5 patients with HFpEF grouped into HFrEF; 1 patient with HFrEF grouped into HFpEF. **D**, Venn diagram of differentially expressed genes (5% false discovery rate threshold) for the 3 groups, their directions versus control, and relative portion unique or shared by each heart failure group. HFpEF indicates heart failure with preserved ejection fraction; HFrEF, heart failure with reduced ejection fraction; and RV, right ventricular.

groups also found both to intermix within their group while remaining segregated from the other groups (Figure V in the Data Supplement).

In total, 8793 genes were differentially expressed between HFpEF and controls and 6802 genes between HFrEF and controls, using a 5% false discovery rate threshold. For each directional change, nearly half were shared, whereas ≈5% went in opposite directions (Figure 1D). Upregulated or downregulated genes in each HF group were subjected to gene ontology and Kyoto Encyclopedia of Genes and Genomes pathway enrichment analysis (Figure VI in the Data Supplement). This identified inflammatory and immune response pathways enriched in both, but uniquely upregulated pathways in HFpEF to be mitochondrial adenosine triphosphate synthesis and oxidative phosphorylation, which were downregulated in HFrEF. Uniquely downregulated HFpEF genes were epigenetic modulators, membrane morphogenesis/organization, organonitrogen signaling, and receptor-coupled kinase signaling, several being upregulated in HFrEF.

HFpEF is proposed to have enhanced oxidative stress, fibrotic, hypertrophic, and inflammatory signaling and depressed nitric oxide and endoplasmic reticular signaling.[28] We therefore examined differential expression between each HF group and controls in these and other selective pathways. Figure 2 plots *Z* scores for genes in each pathway. HFpEF had enhanced expression of oxidative phosphorylation but lower expression of endoplasmic reticular, cGMP-related, autophagy, fibrosis, and hypertrophy-related genes compared with their alterations in HFrEF. Oxidant stress, inflammatory, and nitric oxide signaling pathway genes were similarly affected.

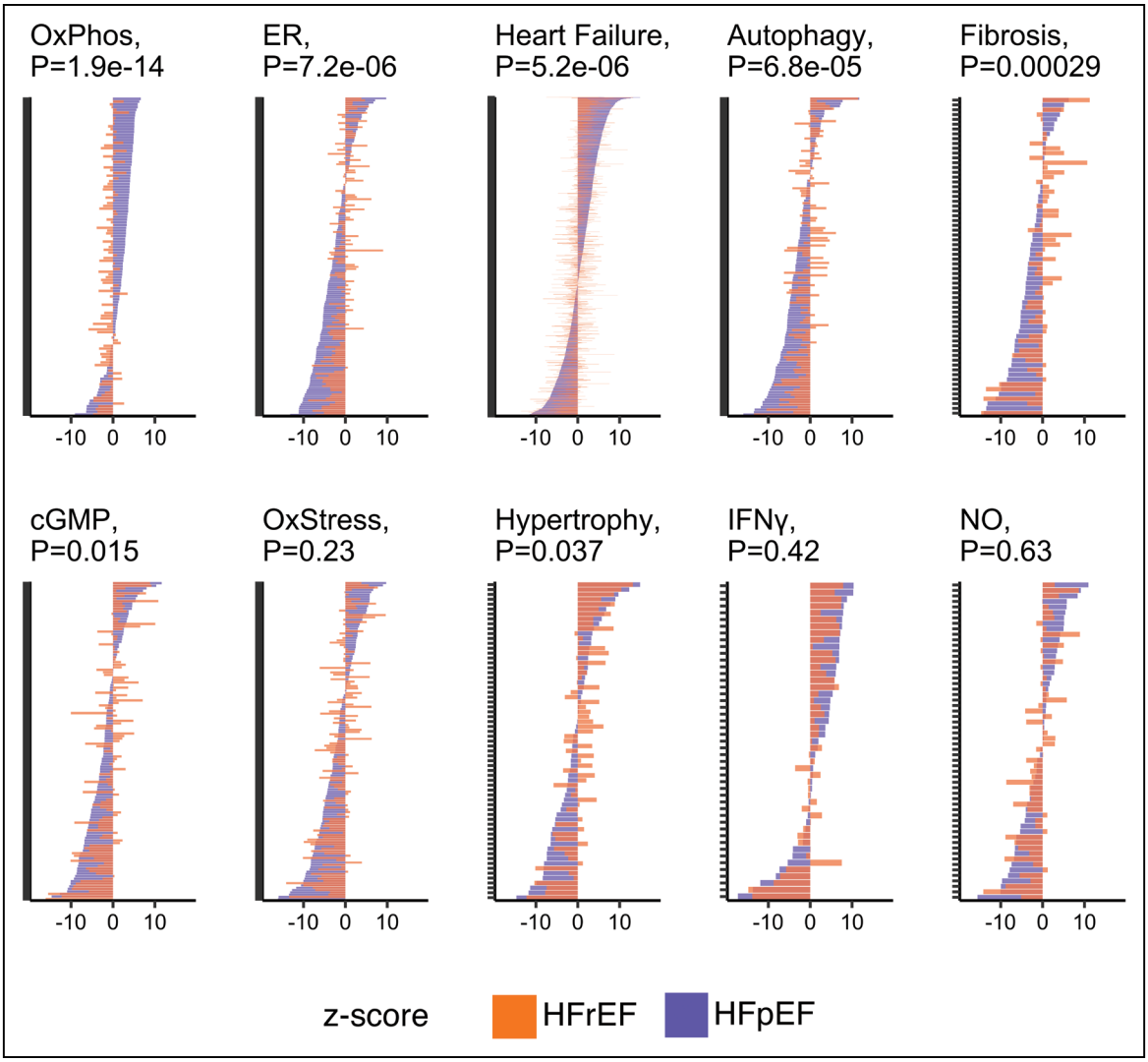

Figure 2. Gene expression differences between HFpEF and HFrEF within targeted pathways of interest.
Gene expression changes in HFpEF versus control (purple) and HFrEF versus control (orange) in 10 targeted pathways. Each plot is displayed as *Z* scores for individual genes. Vertical placement is based on highest to lowest HFpEF versus control scores. Wilcoxon rank-sum *P* value displayed for differences in *Z* scores between heart failure groups. ER indicates protein processing in the endoplasmic reticulum; HFpEF, heart failure with preserved ejection fraction; HFrEF, heart failure with reduced ejection fraction; IFNγ, interferon gamma; NO, nitric oxide; OxPhos, oxidative phosphorylation; and OxStress, oxidative stress.

Influence of HFpEF Covariates on HFpEF Gene Expression Changes

To test the potential influence of major HFpEF morbidities, we repeated pathway analysis of differentially expressed genes obtained after adjusting for clinical covariates within DESeq2, including sex or BMI alone or combined with age, diabetes, and estimated glomerular filtration rate. Downregulated gene-enriched pathways were unchanged despite comorbidity adjustment (Figure 3A). By contrast, upregulated gene pathways were no longer significant after adjusting for all 5 comorbidities and were mostly accounted for by adjusting for BMI alone (Figure 3B). Sex adjustment did not affect pathway enrichment. Thus, the upregulated HFpEF transcriptomic signature is largely associated with obesity but the downregulated one is independent of BMI and other major covariates.

Association of Gene Expression Clusters With HFpEF Clinical Subgroups

Heterogeneity among patients with HFpEF raised the hypothesis that subgroups could be identified solely from their transcriptome that in turn would map to distinctive clinical phenotypes. We tested this using 2 methods. The first was NMF, which identified 3 HFpEF subgroups based on maximal between-patient expression correlations. Groups 1 (n=11) and 2 (n=10) were the most internally correlated, whereas group 3 (n=18) was more heterogeneous (Figure 4A). PCA (using all genes) found group 1 closest to HFrEF (Figure 4B and

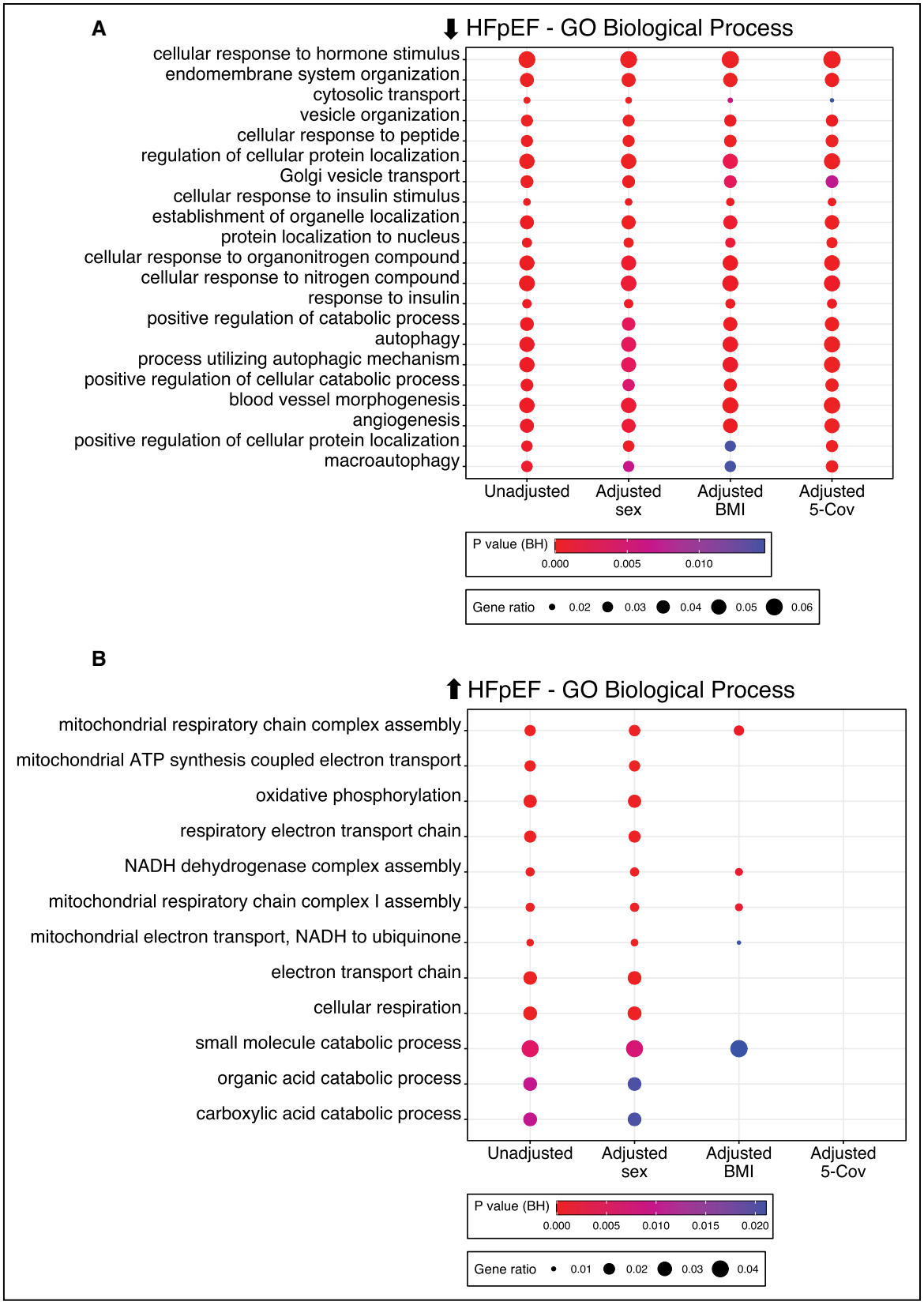

Figure 3. Effect of comorbidities and functional analysis of differentially expressed HFpEF genes.
A, Enrichment of gene ontology (GO)–biological processes based on genes downregulated in HFpEF versus control using unadjusted differential gene expression analysis, adjustment for sex or body mass index (BMI) alone, or adjustment for 5 clinical covariates (age, sex, diabetes, BMI, estimated glomerular filtration rate). Circle size reflects gene ratio: proportion of differentially expressed genes in a pathway versus all differentially expressed genes; color coding reflects Fisher exact *P* value after Benjamini-Hochberg (BH) adjustment for multiple comparisons. **B**, Same analysis using genes upregulated in HFpEF. ATP indicates adenosine triphosphate; HFpEF indicates heart failure with preserved ejection fraction; and NADH, nicotinamide adenine dinucleotide hydride.

Figure VII in the Data Supplement) and the gene pathways enriched in group 1 were shared with patients with HFrEF (Figure 4C). Immune pathways dominated group 2; inflammatory and extracellular matrix processes characterized group 3 (Figure 4C and Figure VIII in the Data Supplement). Table 2 and Table II in the Data Supplement provide clinical features of the 3 groups. Group 1 was predominantly male; nearly all members had diabetes, relatively lower BMI, and higher NT-proBNP, LV dimensions, and pulmonary vascular load. Group 2 was all female; members had the highest BMI, smallest LV size, and lowest NT-proBNP, but higher number of CD68+ inflammatory cells. Time to first event Kaplan-Meier analysis for the first 12 months showed group 1 to have the highest risk of death or HF hospitalization (P=0.025, Figure 4D).

The finding that group 2 contained only women raised the question of whether sex-related differences dominated the transcriptome clustering. We tested this in 2 ways. First, NMF analysis was repeated after removing all genes differentially expressed between HFpEF men and HFpEF women. There were only 96 such genes, including 26 on the X chromosome, and removing them yielded essentially the same NMF result (Figure IXA in the Data Supplement). The second method adjusted for sex in the gene primary reads before NMF processing (Figure IXB in the Data Supplement). This also yielded 3 groups, each fully balanced by sex, but their characteristics remained similar to those of the unadjusted groups (Table III in the Data Supplement).

Whereas NMF identified groups based on optimized gene clusters, we could also examine differentially expressed genes versus controls for each subgroup, focusing on those genes that were not shared by all 3 of the groups. The results (Figures X and XI in the Data Supplement) show oxidative phosphorylation and metabolic processes were similarly upregulated in groups 2 and 3 but not group 1. Immune response pathways were notably downregulated in group 1 but neither other group, whereas autophagy, unfolded protein response, cell growth, and multiple RNA processing pathways were downregulated in groups 2 and 3 but not group 1. Thus, whereas the total HFpEF group exhibited all 3 combined behaviors, this analysis identifies the subsets where these primarily reside.

To further test the robustness of the NMF results, we also employed WGCNA as an alternative method to match transcriptomic groupings with clinical correlates (Figure 5A). These clusters also exhibited morphisms with the groups identified by NMF (Figure 5B and 5C and Table IV in the Data Supplement). NMF group 1 shared many genes with the WGCNA blue cluster that enriched for sarcomere organization and stress-activated kinase signaling pathways and correlated with LV hypertrophy, serum NT-proBNP, and RV afterload. NMF group 2 shared genes in both yellow and red WGCNA clusters in oxidative phosphorylation, immune–inflammatory signaling, and endoplasmic reticulum stress, and patients had opposite clinical features compared with group 1. NMF group 3 matched the brown cluster prominently enriched for extracellular matrix and angiogenesis pathways in patients with smaller, less hypertrophied hearts and less diabetes, but worse HF symptoms.

DISCUSSION

In this first broad analysis of gene expression in myocardium from prospectively identified human patients with HFpEF, we reveal several important findings. First, HFpEF has a distinct transcriptome versus controls and exhibits many unique pathway modifications compared with HFrEF. Second, altered gene expression in pathways often postulated as central to HFpEF pathogenesis including fibrosis, hypertrophy, oxidant stress, and inflammation[29] are similar or less augmented compared with HFrEF, whereas more unique pathways in HFpEF relate to protein hemostasis, endoplasmic reticulum stress, and angiogenesis. Third, HFpEF can be subgrouped based solely on transcriptomics, yielding (1) a hemodynamic-driven phenotype that shares similarities to HFrEF and has worse clinical outcomes; (2) a cohort with smaller hearts and inflammatory and matrix signatures; and (3) a heterogeneous phenotype with worse HF symptoms but lower NT-proBNP and smaller hearts as well. This remains distinct from HFrEF. These relations between underlying transcriptomic signatures and their clinical correlates suggests a path forward for more personalized and biologically based therapeutics.

HFpEF Displays Broad Transcriptomic Changes Despite Clinical Heterogeneity

Initial reports of HFpEF in the 1980s (termed diastolic heart failure at the time) described mostly elderly, hypertensive, and predominantly female patients with hypertrophied ventricles without obvious coronary disease.[4] This remained a primary phenotype over the next 20 years, with hypertension, hypertrophy, fibrosis, and resulting diastolic impairment considered the primary disease pathophysiology. The phenotype has changed over the past 2 decades to involve a younger, mixed-sex population, characterized by severe obesity and metabolic comorbidities.[6,8] This evolution has shifted the mechanistic perspective to a multiorgan disease[9] that includes pulmonary hypertension, obesity and metabolic disease, vascular stiffening, chronotropic incompetence, skeletal muscle disease, and renal insufficiency.[30] In this context, the role of the heart has become more ambiguous, and although suspicions persist that the myocardium is not normal, the way in which the myocardium is not normal is less certain.

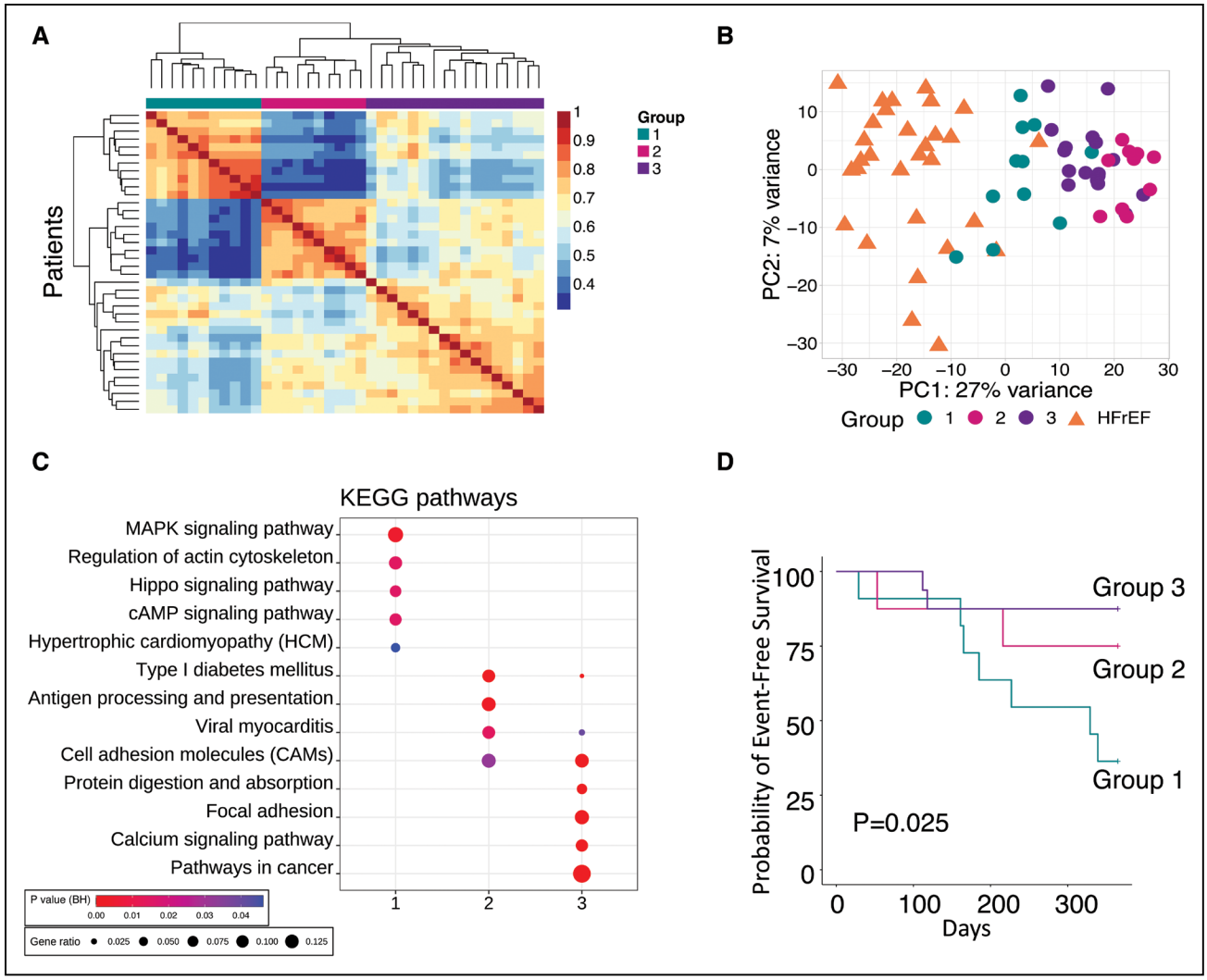

Figure 4. Identification of HFpEF subgroups, by agnostic clustering of gene expression.
A, Non–negative matrix factorization identifies 3 HFpEF patient clusters (n=38). Two groups show high intragroup similarity; the third is heterogeneous. **B**, Principal component (PC) analysis using HFpEF groups and heart failure with reduced ejection fraction (HFrEF) as comparator. **C**, Enrichment of Kyoto Encyclopedia of Genes and Genomes (KEGG) pathways in the subset of differentially expressed genes within HFpEF subgroups. **D**, Kaplan-Meier analysis of 12-month probability of event-free survival, with event being a composite of death or heart failure hospitalization. Log-rank *P* value displayed. BH indicates Benjamini-Hochberg; HFpEF, heart failure with preserved ejection fraction**;** and MAPK, mitogen-activated protein kinase.

This heterogeneity has been blamed for clinical failures of therapeutic trials.[31]

In this context, a coherent HFpEF transcriptomic profile despite clinical heterogeneity is intriguing and reveals shared myocardial signaling distinct from controls or HFrEF. The variance in individual gene expression among patients with HFpEF was relatively modest and similar to that in patients with HFrEF and controls, even though the latter are often considered less clinically heterogeneous. Given the larger size of our HFpEF cohort, we were able for the first time to further dissect out myocardial molecular subgroups. We know of only 1 previous report of myocardial transcriptomics from 16 patients undergoing coronary bypass surgery, 5 of whom had HFpEF features.[32] None of the 5 was prospectively identified with clinical HF and only 1 was treated with a diuretic (none a loop diuretic), limiting interpretability of the data. By contrast, the current results are derived from a well-characterized cohort of symptomatic patients with HFpEF under active medical management.

HFpEF Transcriptomic Signatures and the Role of Comorbidities

Previous studies have proposed various pathophysiologic components thought to underlie HFpEF, including myocyte hypertrophy, interstitial fibrosis, oxidative stress, and abnormal nitric oxide signaling.[29] Although we found these pathways more engaged in HFpEF compared with controls, similar if not greater changes were found in HFrEF; they are thus not unique to HFpEF. By contrast, several pathways dysregulated in HFpEF versus controls differed from those observed in late-stage

Table 2. Clinical Characteristics of 3 HFpEF Groups Derived by Non–Negative Matrix Factorization

Variable	Group 1 (11)	Group 2 (10)	Group 3 (17)	*P* value
Age, y	62 (53, 72)	64 (44, 68)	61 (56, 67)	0.77
Female	4 (36)**	10 (100)†††	7 (41)	0.002
HF hospitalization past 12 months	9 (82)	6 (60)	12 (71)	0.53
NYHA class				0.079
II	3 (27)	1 (10)	9 (53)	
III	8 (73)	8 (80)	8 (47)	
IV	0 (0)	1 (10)	0 (0)	
Medical history				
Hypertension	11 (100)	9 (90)	17 (100)	0.26
Diabetes	10 (91)†	6 (60)	9 (53)	0.1
Coronary artery disease	0 (0)	2 (20)	2 (12)	0.26
Atrial fibrillation/flutter	4 (36)	0 (0)	6 (35)	0.083
Systolic BP, mm Hg	141 (138, 173)	136 (125, 161)	136 (124, 147)	0.31
Diastolic BP, mm Hg	68 (65, 80)	74 (61, 82)	75 (66, 79)	0.97
BMI, kg/m^2	37 (33, 46)	43 (41, 48)	41 (36, 46)	0.26
eGFR, mL/min/1.73 m^2	38 (30, 68)	51 (44, 96)	49 (33, 70)	0.32
BUN, mg/dL	38 (22, 52)*	18 (15, 24)	22 (17, 29)	0.043
Creatinine, mg/dL	1.90 (1.20, 2.15)*	1.25 (0.85, 1.30)	1.40 (1.10, 2.30)	0.09
NT-proBNP, pg/mL	1505 (418, 3279)***, †	48 (28, 92)††	169 (113, 591)	<0.001
Echocardiography				
LVEF, %	60 (55, 65)	65 (61, 69)	65 (65, 70)	0.19
LVEDD, cm	4.8 (4.2, 5.7)*	4.0 (3.7, 4.3)††	4.9 (4.2, 5.1)	0.005
LA diameter, cm	4.4 (3.8, 5.0)	3.8 (3.3, 4.2)†	4.3 (3.8, 4.7)	0.075
Sex-adjusted LV mass/height$^{1.7}$, g/m$^{1.7}$	114 (95, 151)	98 (69, 123)	98 (83, 116)	0.21
LV mass index, g/m^2	121 (109, 134)**, †	74 (55, 93)	93 (85, 113)	0.005
Invasive hemodynamics				
RAP, mm Hg	13 (8, 16)	11 (8, 15)	12 (9, 14)	0.91
PASP, mm Hg	54 (50, 67)*, ††	41 (32, 49)	43 (33, 48)	0.006
PA mean, mm Hg	34 (29, 38)†	29 (22, 35)	28 (23, 32)	0.074
PAWP, mm Hg	21 (16, 26)	19 (13, 24)	20 (16, 22)	0.73
Cardiac index, L/min/m^2	3.00 (2.20, 3.48)	2.51 (2.27, 3.02)	2.49 (2.40, 2.64)	0.75
PVR, WU	2.73 (1.57, 3.45)	1.48 (1.25, 2.27)	1.58 (0.89, 2.09)	0.11
PVR ≥3 WU	4 (36)	0 (0)	1 (5.9)	0.031
RVSWI, g/m^2/beat	9.7 (9.1, 11.9)*	7.6 (5.5, 8.9)	7.0 (5.7, 9.5)	0.043
Transpulmonary gradient, mm Hg	12.0 (11.5, 20.0)*, †	8.0 (7.2, 11.0)	8.0 (7.0, 11.0)	0.023
PA compliance, mL/mm Hg	2.4 (1.8, 3.9)*, †	3.9 (3.6, 4.4)	4.3 (3.0, 5.0)	0.048
Clinical histology				
% Fibrosis	7.2 (5.7, 7.6)	5.0 (3.4, 10.1)	8.0 (7.1, 11.1)	0.29
CD68 cells/mm^2	40 (29, 55)*	80 (51, 99)	61 (38, 107)	0.094

Data presented as n (%) or median (25th, 75th percentile). Fisher exact test used for categorical variables. Kruskal-Wallis test used for continuous variables. *P<0.05 vs group 2, **P≤0.01 vs group 2, ***P≤0.001 vs group 2; †P<0.05 vs group 3, ††P≤0.01 vs group 3, †††P≤0.001 vs group 3. BMI indicates body mass index; BP, blood pressure; eGFR, estimated glomerular filtration rate; HFpEF, heart failure with preserved ejection fraction; LA, left atrial; LV, left ventricular; LVEDD, left ventricular end-diastolic diameter; LVEF, left ventricular ejection fraction; NT-proBNP, N-terminal pro–B-type natriuretic peptide; NYHA, New York Heart Association; PA, pulmonary artery; PASP, pulmonary artery systolic pressure; PAWP, pulmonary artery wedge pressure; PVR, pulmonary vascular resistance; RAP, right atrial pressure; and RVSWI, right ventricular stroke work index.

HFrEF. The upregulation of genes in oxidative phosphorylation/adenosine triphosphate synthesis pathways is intriguing given that they are downregulated in HFrEF and this pathway enrichment is linked with differences in BMI between HFpEF and controls. Obesity engages a complex pathophysiology involving adipokines, vascular

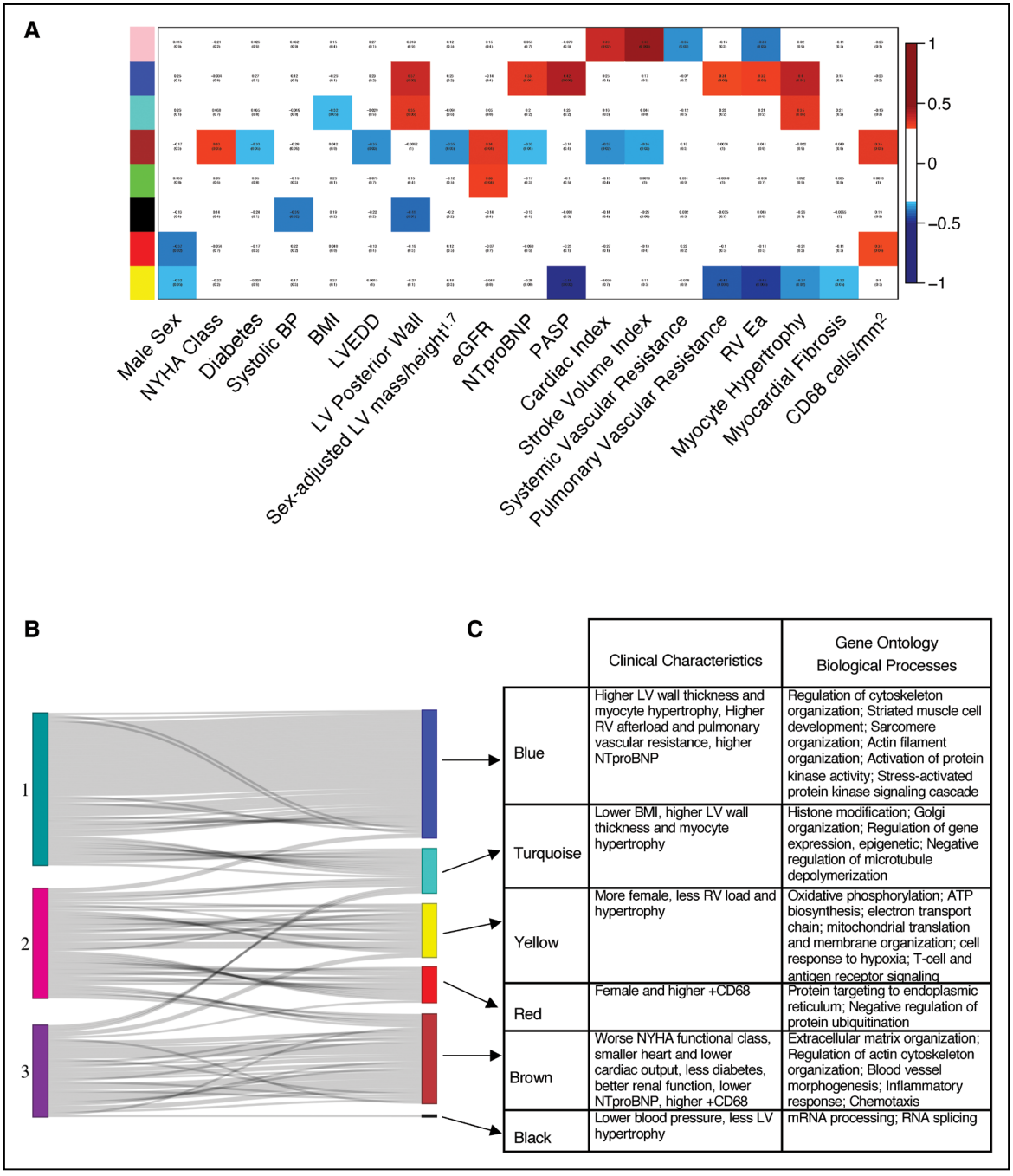

	Clinical Characteristics	Gene Ontology Biological Processes
Blue	Higher LV wall thickness and myocyte hypertrophy, Higher RV afterload and pulmonary vascular resistance, higher NTproBNP	Regulation of cytoskeleton organization; Striated muscle cell development; Sarcomere organization; Actin filament organization; Activation of protein kinase activity; Stress-activated protein kinase signaling cascade
Turquoise	Lower BMI, higher LV wall thickness and myocyte hypertrophy	Histone modification; Golgi organization; Regulation of gene expression, epigenetic; Negative regulation of microtubule depolymerization
Yellow	More female, less RV load and hypertrophy	Oxidative phosphorylation; ATP biosynthesis; electron transport chain; mitochondrial translation and membrane organization; cell response to hypoxia; T-cell and antigen receptor signaling
Red	Female and higher +CD68	Protein targeting to endoplasmic reticulum; Negative regulation of protein ubiquitination
Brown	Worse NYHA functional class, smaller heart and lower cardiac output, less diabetes, better renal function, lower NTproBNP, higher +CD68	Extracellular matrix organization; Regulation of actin cytoskeleton organization; Blood vessel morphogenesis; Inflammatory response; Chemotaxis
Black	Lower blood pressure, less LV hypertrophy	mRNA processing; RNA splicing

Figure 5. WGCNA in HFpEF.
A, WGCNA identified 8 gene clusters, represented as colors on the y-axis. Their correlation with clinical measures is shown as red boxes indicating positive and blue boxes negative correlations. **B**, The top 300 metagenes inherent to non–negative matrix factorization (NMF) group 1 HFpEF overlap significantly with the blue cluster from the WGCNA. Each line represents a gene in an NMF group that best defined that group and its match among the gene clusters identified by WGCNA. Genes from HFpEF group 1 overlap most with the blue cluster, genes from group 2 mostly overlap with the yellow and red clusters, and group 3 mostly overlaps with the brown cluster. **C**, Table identifies the clinical characteristics and gene ontology biological processes related to each group. ATP indicates adenosine triphosphate; BMI, body mass index; BP, blood pressure; eGFR, estimated glomerular filtration rate; HFpEF, heart failure with preserved ejection fraction; LV, left ventricular; LVEDD, left ventricular end diastolic diameter; NT-proBNP, N-terminal pro–B-type natriuretic peptide; NYHA, New York Heart Association; PASP, pulmonary artery systolic pressure; RV Ea, right ventricle arterial elastance; and WGCNA, weighted gene correlation network analysis.

dysfunction, inflammatory signaling, metabolic fuel use defects, and many other features that contribute to cardiometabolic syndromes.[33,34] It is possible that upregulated energy-related genes in more obese patients with HFpEF relate to this pathobiology, but it could also reflect higher energy requirements to perfuse more tissue (fat) than the heart was designed for and to handle the increased workload attributable to higher inertance to movement. This may need to be dissected using cardiometabolic preclinical models because myocardial

tissue from obese patients with nonfailing hearts will be difficult to obtain.

Equally interesting is the set of genes uniquely downregulated in HFpEF that could not be accounted for by BMI or other major comorbidities. These genes involve protein homeostasis, trafficking, angiogenesis, endoplasmic reticulum processing and stress, and protein recycling. They were consistently identified using different bioinformatics methods, including gene ontology, Kyoto Encyclopedia of Genes and Genomes, NMF, and WGCNA. The presence of depressed endoplasmic reticulum processing genes is notable in light of data from a carefully phenotyped mouse HFpEF model combining hemodynamic and metabolic stress that found the pathway is depressed and biologically relevant.[35] Confirmation of its functional relevance in larger mammals and particular humans with HFpEF awaits future studies. It is important to recognize that gene expression does not imply functional effects or necessarily correlate with protein levels, but it puts a spotlight on pathways likely to be engaged. Further studies are needed to test various candidates as therapeutic targets.

Identifying HFpEF Subgroups by the Transcriptome

Many recent studies have used a broad array of clinical data including serum biomarkers to phenotype HFpEF subgroups by artificial intelligence/machine learning and cluster-mapping approaches.[31,36,37] These find that patients with HFpEF at highest risk generally have right heart dysfunction, hemodynamic overload, higher NT-proBNP, and often renal dysfunction.[31,36,37] Whether or how these groups map to molecular signatures was previously unknown, but the new data suggest they are. A limiting factor is that patients with HFpEF often present with many overlapping features, making it difficult to assign them to predesignated clinical subgroups. Here, we took the opposite approach, using only the transcriptome to develop subgroup clusters, then mapping the clusters back to clinical features and biological pathways. Despite the inherent mathematical differences in NMF and WGCNA analyses, we found remarkable concordance between NMF group 1, an agnostically identified high-risk subgroup that shares features of the high-risk cohorts in prior clinical–phenomapping studies,[31,36,37] and the WGCNA blue module, suggesting biological relevance. Interestingly, the transcriptome of this subgroup is also closest to HFrEF, suggesting therapies for the latter may benefit this HFpEF subgroup. By contrast, therapies targeting protein processing, metabolism, inflammation, or matrix remodeling may more benefit NMF groups 2 or 3; obesity reduction would likely help all groups.

Limitations

Our study has several limitations. The results do not test a specific mechanism for HFpEF, but rather provide a framework for biological exploration of the syndrome. We used whole myocardial rather than single cell RNAseq, as the latter has yet to be established from heart biopsies; thus, cell-specific expression remains to be clarified. The patients with HFrEF had late-stage disease and were being transplanted, and whereas this may reflect more severe disease than the HFpEF cohort, the latter group had well-documented hemodynamics, functional class, HF hospitalization rates, and disability representing a high morbidity clinical phenotype. Furthermore, the majority of molecular and cellular data for human HF derives from tissue procured in advanced HFrEF in the same manner. The control tissue from brain-dead organ donors may be affected by the conditions surrounding death; however, the within-group transcriptomes were consistent. We were limited to the unused donor and HFrEF explant tissue available and were not able to match patients based on demographics and comorbidities. The myocardial tissue in HFpEF is from the RV septum, the standard sampling location for endomyocardial biopsy, and although we cannot be certain gene expression is identical in the LV in HFpEF, we found strong transcriptomic agreement between tissue from the LV and RV in patients with HFrEF that was unaltered by RV load from pulmonary hypertension.

CONCLUSIONS

HFpEF myocardium displays characteristic transcriptional signatures, distinct from controls and HFrEF. Some of these transcriptome signatures are closely linked to obesity and other comorbidities, whereas others are not. We find molecular subgroups within HFpEF have corresponding distinctive clinical profiles. Together, these results provide new biological insights into HFpEF and help forge a framework to develop better precision-guided therapeutics.

ARTICLE INFORMATION

Received July 31, 2020; accepted October 22, 2020.

The Data Supplement, podcast, and transcript are available with this article at https://www.ahajournals.org/doi/suppl/10.1161/circulationaha.120.050498.

Correspondence

David A. Kass, MD, Abraham and Virginia Weiss Professor of Cardiology, Professor of Medicine, Biomedical Engineering and Pharmacology and Molecular Sciences, The Johns Hopkins University School of Medicine, Ross Research Building, Room 858, 720 Rutland Avenue, Baltimore, MD 21205; or Kavita Sharma, MD, Assistant Professor of Medicine, Director, Advanced Heart Failure and Cardiac Transplantation; Director, Johns Hopkins University Heart Failure With Preserved Ejection Fraction Program, The Johns Hopkins Hospital, 600 North Wolfe Street, Carnegie 568B, Baltimore, MD 21287. Email dkass@jhmi.edu or ksharma8@jhmi.edu

Affiliations

Division of Cardiology, Johns Hopkins University School of Medicine, Baltimore, MD (V.S.H., J.V., D.A.K., K.S.). Department of Biomedical Engineering, Johns Hopkins University, Baltimore, MD (H.K., J.S.B., D.A.K.). Genome Analysis Unit, Amgen Research, San Francisco, CA (X.L., J.Y.). Division of Cardiology, University of Pennsylvania, Philadelphia (K.B., K.B.M.). Cardiometabolic Disorders Research, Amgen Research, San Francisco, CA (S.M.H., A.Y.K.). Cardiometabolic Disorders Research, Amgen Research, Thousand Oaks, CA (M.S.). Calico Life Sciences, San Francisco, CA (A.Y.K.).

Sources of Funding

NextGen RNA sequencing was supported by a research grant from Amgen, Inc. Dr Kass was supported by American Heart Association grant 16SFRN28620000 and National Heart, Lung, and Blood Institute grant R35-HL135827. Dr Sharma was supported by American Heart Association grant 16SFRN27870000, National Heart, Lung, and Blood Institute grant R01-HL61912, and Johns Hopkins University School of Medicine Clinician Scientist Award. Dr Hahn was supported by National Institutes of Health grant 2T32HL007227-44; Drs Bader and Knutsdottir were supported by National Heart, Lung, and Blood Institute grant R35-HL135827; and Dr Margulies was supported by a research grant from Sanofi-Aventis. Drs Luo, Haldar, and Stolina are employees of Amgen, Inc. Drs Yin and Khakoo were employees of Amgen when the project started and have since left the company.

Disclosures

Drs Hahn, Knutsdottir, Marguiles, and Vaishnav, and K. Bedi report no disclosures. Drs. Luo, Haldar, and Stolina are employees and stockholders of Amgen, Inc; Drs. Yin and Khakoo were employees of Amgen when the project started and have since left the company. Dr Bader is a founder and director of Neochromosome. Dr Kass is a consultant and Scientific Advisory Board Member (Cardiometabolic) for Amgen. Dr Haldar is an executive, officer, and shareholder of Amgen and is a scientific founder and shareholder of Tenaya Therapeutics. Dr Khakoo is a full-time employee of Calico Life Sciences, LLC. Dr Sharma is a consultant and advisory board member and receives honoraria from Novartis, Janssen, Bayer, and Bristol Myers Squibb.

Supplemental Materials

Data Supplement Figures I–XI
Data Supplement Tables I–IV

REFERENCES

1. Benjamin EJ, Virani SS, Callaway CW, Chamberlain AM, Chang AR, Cheng S, Chiuve SE, Cushman M, Delling FN, Deo R, et al; American Heart Association Council on Epidemiology and Prevention Statistics Committee and Stroke Statistics Subcommittee. Heart disease and stroke statistics: 2018 update: a report from the American Heart Association. *Circulation.* 2018;137:e67–e492. doi: 10.1161/CIR.0000000000000558
2. Owan TE, Hodge DO, Herges RM, Jacobsen SJ, Roger VL, Redfield MM. Trends in prevalence and outcome of heart failure with preserved ejection fraction. *N Engl J Med.* 2006;355:251–259. doi: 10.1056/NEJMoa052256
3. Sharma K, Hill T, Grams M, Daya NR, Hays AG, Fine D, Thiemann DR, Weiss RG, Tedford RJ, Kass DA, et al. Outcomes and worsening renal function in patients hospitalized with heart failure with preserved ejection fraction. *Am J Cardiol.* 2015;116:1534–1540. doi: 10.1016/j.amjcard.2015.08.019
4. Topol EJ, Traill TA, Fortuin NJ. Hypertensive hypertrophic cardiomyopathy of the elderly. *N Engl J Med.* 1985;312:277–283. doi: 10.1056/NEJM198501313120504
5. Borbély A, van der Velden J, Papp Z, Bronzwaer JG, Edes I, Stienen GJ, Paulus WJ. Cardiomyocyte stiffness in diastolic heart failure. *Circulation.* 2005;111:774–781. doi: 10.1161/01.CIR.0000155257.33485.6D
6. Kitzman DW, Shah SJ. The HFpEF obesity phenotype: the elephant in the room. *J Am Coll Cardiol.* 2016;68:200–203. doi: 10.1016/j.jacc.2016.05.019
7. Kitzman DW, Nicklas BJ. Pivotal role of excess intra-abdominal adipose in the pathogenesis of metabolic/obese HFpEF. *JACC Heart Fail.* 2018;6:1008–1010. doi: 10.1016/j.jchf.2018.08.007
8. Obokata M, Reddy YNV, Pislaru SV, Melenovsky V, Borlaug BA. Evidence supporting the existence of a distinct obese phenotype of heart failure with preserved ejection fraction. *Circulation.* 2017;136:6–19. doi: 10.1161/circulationaha.116.026807
9. Sharma K, Kass DA. Heart failure with preserved ejection fraction: mechanisms, clinical features, and therapies. *Circ Res.* 2014;115:79–96. doi: 10.1161/CIRCRESAHA.115.302922
10. Zile MR, Baicu CF, Ikonomidis JS, Stroud RE, Nietert PJ, Bradshaw AD, Slater R, Palmer BM, Van Buren P, Meyer M, et al. Myocardial stiffness in patients with heart failure and a preserved ejection fraction: contributions of collagen and titin. *Circulation.* 2015;131:1247–1259. doi: 10.1161/CIRCULATIONAHA.114.013215
11. Westermann D, Lindner D, Kasner M, Zietsch C, Savvatis K, Escher F, von Schlippenbach J, Skurk C, Steendijk P, Riad A, et al. Cardiac inflammation contributes to changes in the extracellular matrix in patients with heart failure and normal ejection fraction. *Circ Heart Fail.* 2011;4:44–52. doi: 10.1161/CIRCHEARTFAILURE.109.931451
12. van Heerebeek L, Hamdani N, Falcão-Pires I, Leite-Moreira AF, Begieneman MP, Bronzwaer JG, van der Velden J, Stienen GJ, Laarman GJ, Somsen A, et al. Low myocardial protein kinase G activity in heart failure with preserved ejection fraction. *Circulation.* 2012;126:830–839. doi: 10.1161/CIRCULATIONAHA.111.076075
13. Runte KE, Bell SP, Selby DE, Haussler TN, Ashikaga T, LeWinter MM, Palmer BM, Meyer M. Relaxation and the role of calcium in isolated contracting myocardium from patients with hypertensive heart disease and heart failure with preserved ejection fraction. *Circ Heart Fail.* 2017;10:e004311. doi: 10.1161/CIRCHEARTFAILURE.117.004311
14. Hahn VS, Knutsdottir H, Luo X, Bedi KC Jr, Margulies KB, Haldar SM, Stolina M, Yin J, Khakoo AY, Vaishnav J, et al. Myocardial gene expression signatures in human heart failure with preserved ejection fraction. *Zenodo Data Repository.* 2020. doi: 10.5281/zenodo.4114617
15. Pieske B, Tschöpe C, de Boer RA, Fraser AG, Anker SD, Donal E, Edelmann F, Fu M, Guazzi M, Lam CSP, et al. How to diagnose heart failure with preserved ejection fraction: the HFA-PEFF diagnostic algorithm: a consensus recommendation from the Heart Failure Association (HFA) of the European Society of Cardiology (ESC). *Eur J Heart Fail.* 2020;22:391–412. doi: 10.1002/ejhf.1741
16. Ponikowski P, Voors AA, Anker SD, Bueno H, Cleland JGF, Coats AJS, Falk V, González-Juanatey JR, Harjola VP, Jankowska EA, et al; ESC Scientific Document Group. 2016 ESC guidelines for the diagnosis and treatment of acute and chronic heart failure: the task force for the diagnosis and treatment of acute and chronic heart failure of the European Society of Cardiology (ESC): developed with the special contribution of the Heart Failure Association (HFA) of the ESC. *Eur Heart J.* 2016;37:2129–2200. doi: 10.1093/eurheartj/ehw128
17. Yancy CW, Jessup M, Bozkurt B, Butler J, Casey DE Jr, Drazner MH, Fonarow GC, Geraci SA, Horwich T, Januzzi JL, et al. 2013 ACCF/AHA guideline for the management of heart failure: executive summary: a report of the American College of Cardiology Foundation/American Heart Association task force on practice guidelines. *Circulation.* 2013;128:1810–1852. doi: 10.1161/CIR.0b013e31829e8807
18. McKee PA, Castelli WP, McNamara PM, Kannel WB. The natural history of congestive heart failure: the Framingham study. *N Engl J Med.* 1971;285:1441–1446. doi: 10.1056/NEJM197112232852601
19. Lang RM, Badano LP, Mor-Avi V, Afilalo J, Armstrong A, Ernande L, Flachskampf FA, Foster E, Goldstein SA, Kuznetsova T, et al. Recommendations for cardiac chamber quantification by echocardiography in adults: an update from the American Society of Echocardiography and the European Association of Cardiovascular Imaging. *J Am Soc Echocardiogr.* 2015;28:1–39.e14. doi: 10.1016/j.echo.2014.10.003
20. Hahn VS, Yanek LR, Vaishnav J, Ying W, Vaidya D, Lee YZJ, Riley SJ, Subramanya V, Brown EE, Hopkins CD, et al. Endomyocardial biopsy characterization of heart failure with preserved ejection fraction and prevalence of cardiac amyloidosis. *JACC Heart Fail.* 2020;8:712–724. doi: 10.1016/j.jchf.2020.04.007
21. Kim D, Langmead B, Salzberg SL. HISAT: a fast spliced aligner with low memory requirements. *Nat Methods.* 2015;12:357–360. doi: 10.1038/nmeth.3317
22. Anders S, Pyl PT, Huber W. HTSeq: a Python framework to work with high-throughput sequencing data. *Bioinformatics.* 2015;31:166–169. doi: 10.1093/bioinformatics/btu638
23. Love MI, Huber W, Anders S. Moderated estimation of fold change and dispersion for RNA-seq data with DESeq2. *Genome Biol.* 2014;15:550. doi: 10.1186/s13059-014-0550-8

24. Langfelder P, Horvath S. WGCNA: an R package for weighted correlation network analysis. *BMC Bioinformatics.* 2008;9:559. doi: 10.1186/1471-2105-9-559
25. Gaujoux R, Seoighe C. A flexible R package for nonnegative matrix factorization. *BMC Bioinformatics.* 2010;11:367. doi: 10.1186/1471-2105-11-367
26. Brunet JP, Tamayo P, Golub TR, Mesirov JP. Metagenes and molecular pattern discovery using matrix factorization. *Proc Natl Acad Sci U S A.* 2004;101:4164–4169. doi: 10.1073/pnas.0308531101
27. Johnson EK, Matkovich SJ, Nerbonne JM. Regional differences in mRNA and lncRNA expression profiles in non-failing human atria and ventricles. *Sci Rep.* 2018;8:13919. doi: 10.1038/s41598-018-32154-2
28. Paulus WJ. Unfolding discoveries in heart failure. *N Engl J Med.* 2020;382:679–682. doi: 10.1056/NEJMcibr1913825
29. Paulus WJ, Tschöpe C. A novel paradigm for heart failure with preserved ejection fraction: comorbidities drive myocardial dysfunction and remodeling through coronary microvascular endothelial inflammation. *J Am Coll Cardiol.* 2013;62:263–271. doi: 10.1016/j.jacc.2013.02.092
30. Shah SJ, Borlaug BA, Kitzman DW, McCulloch AD, Blaxall BC, Agarwal R, Chirinos JA, Collins S, Deo RC, Gladwin MT, et al. Research priorities for heart failure with preserved ejection fraction: National Heart, Lung, and Blood Institute working group summary. *Circulation.* 2020;141:1001–1026. doi: 10.1161/CIRCULATIONAHA.119.041886
31. Shah SJ, Katz DH, Selvaraj S, Burke MA, Yancy CW, Gheorghiade M, Bonow RO, Huang CC, Deo RC. Phenomapping for novel classification of heart failure with preserved ejection fraction. *Circulation.* 2015;131:269–279. doi: 10.1161/CIRCULATIONAHA.114.010637
32. Das S, Frisk C, Eriksson MJ, Walentinsson A, Corbascio M, Hage C, Kumar C, Asp M, Lundeberg J, Maret E, et al. Transcriptomics of cardiac biopsies reveals differences in patients with or without diagnostic parameters for heart failure with preserved ejection fraction. *Sci Rep.* 2019;9:3179. doi: 10.1038/s41598-019-39445-2
33. Collins S. A heart-adipose tissue connection in the regulation of energy metabolism. *Nat Rev Endocrinol.* 2014;10:157–163. doi: 10.1038/nrendo.2013.234
34. Koliaki C, Liatis S, Kokkinos A. Obesity and cardiovascular disease: revisiting an old relationship. *Metabolism.* 2019;92:98–107. doi: 10.1016/j.metabol.2018.10.011
35. Schiattarella GG, Altamirano F, Tong D, French KM, Villalobos E, Kim SY, Luo X, Jiang N, May HI, Wang ZV, et al. Nitrosative stress drives heart failure with preserved ejection fraction. *Nature.* 2019;568:351–356. doi: 10.1038/s41586-019-1100-z
36. Cohen JB, Schrauben SJ, Zhao L, Basso MD, Cvijic ME, Li Z, Yarde M, Wang Z, Bhattacharya PT, Chirinos DA, et al. Clinical phenogroups in heart failure with preserved ejection fraction: detailed phenotypes, prognosis, and response to spironolactone. *JACC Heart Fail.* 2020;8:172–184. doi: 10.1016/j.jchf.2019.09.009
37. Segar MW, Patel KV, Ayers C, Basit M, Tang WHW, Willett D, Berry J, Grodin JL, Pandey A. Phenomapping of patients with heart failure with preserved ejection fraction using machine learning-based unsupervised cluster analysis. *Eur J Heart Fail.* 2020;22:148–158. doi: 10.1002/ejhf.1621